EAI Endorsed Transactions
on Transportation Systems and Ocean Engineering Research Article EAI.EU

# Integrating model predictive control with deep learning for sway reduction in ship-to-shore crane operations

Xuan-Kien Dang[1], Viet-Dung Do[1,*], Ngoc-Truc Nguyen[1], and Soi-Ly[1]

[1]AIT Research Group, Ho Chi Minh City University of Transport, Vietnam

## Abstract

The sway of the container winch drive system results in significant nonlinearity in Ship-to-Shore (STS) crane operations. As a result, achieving an accurate winch path becomes challenging, raising safety concerns for the operator and increasing the risk of accidents to both goods and equipment. This paper presents a Deep learning-based Model Predictive Control (DMPC) designed to improve the precision of the winch control signal during STS operations, ultimately reducing the load sway amplitude. First, a Long Short-Term Memory (LSTM) is employed to compute a state prediction model that forecasts the load sway angle and winch displacement amplitude. The predicted state $\hat{x}(k+1)$ serves as input to the DMPC controller, which determines the winch control value through an optimization function. Finally, the proposed solution is tested through two scenarios, yielding promising results that demonstrate its effectiveness.

**Keywords:** deep learning, model predictive control, prediction model, ship-to-shore crane, sway angle.

Received on 08 November 2025, accepted on 12 December 2025, published on 15 December 2025



doi: 10.4108/_____

## 1. Introduction

Ship-to-shore (STS) cranes are widely used for transferring cargo between vessels and the quay, employing wire ropes and a mechanical spreader frame. The crane operates by lowering the boom to a horizontal position during handling, allowing for the transfer of containers from ship to shore and vice versa. Containers are secured via the hatch cover and spreader frame. In contrast, the main hoist and trolley can operate simultaneously under winds below 20 m/s. However, the drive system is sensitive to external disturbances such as wind and irregular trolley motion, which often cause undesirable load sway. This sway reduces operational efficiency, increases the time required to suppress oscillations, and poses safety risks. The high sway leads to collisions with structures or personnel, causing equipment damage and accidents. In severe cases, crane structural components could be compromised, potentially leading to tilting or collapse. To address these issues, manufacturers adopt control solutions focused on operational improvement.

Many studies aim to apply modern techniques to mitigate load sway in container crane operations. Zhang *et al.* [1] developed a partially saturated nonlinear controller for underactuated overhead cranes, based on passivity and energy-shaping methods. Their approach constructs an assignable storage function characterized by a desired damping matrix and, notably, quadratic in a newly defined coupled error vector. Additionally, linear control strategies have also been extensively investigated. Lu *et al.* [2] proposed a sliding mode control method, which guarantees satisfactory control performance even when the crane operates under adverse conditions. Moreover, to mitigate the inherent chattering of sliding mode control, a disturbance observer has been designed for overhead cranes to estimate and subsequently eliminate the effects of external disturbances. Chen *et al.* [3] proposed an adaptive tracking control method that achieves effective tracking

*Corresponding author. Email: dungdv@ut.edu.vn

performance in the presence of parameter uncertainties and external perturbations. Specifically, by exploiting passivity properties, an energy-like shaped function was designed as a Lyapunov candidate, upon which an adaptive tracking controller was developed to handle parameter uncertainties. A typical phenomenon in large-scale cranes, such as gantry cranes, is the occurrence of lateral structural vibrations caused by trolley motion and the limited stiffness of the crane structure. These structural oscillations interact with load sway and therefore must be considered in any control design process. In practical conditions, the optimal control force was addressed [4-5], ensuring a robust control signal [6-7]. However, structural vibrations of the crane are only partially attenuated, which has motivated the design and implementation of advanced control strategies such as model predictive control (MPC) [8-9]. In particular, a novel control approach based on multivariable MPC combined with particle swarm optimization has been proposed to suppress both transient oscillations and residual vibrations of the payload handled by overhead cranes.

**Figure 1.** Operations of the STS cranes at Tan Cang – Cat Lai port, Vietnam

In recent years, artificial intelligence [10-11] and deep learning [12] have developed new approaches to address complex control and operational challenges. These technical problems are effectively fixed through advanced analytical techniques applied to large datasets. Some studies have built upon theoretical achievements in related fields such as big data. While the others have proposed sustainable practical applications in the transportation aspect, particularly for optimizing delays and reducing various prediction errors [13-14]. Zhang *et al.* [15] developed a model-independent control method, termed derivative-proportional sliding mode control, to achieve simultaneous trolley positioning and load sway suppression in gantry cranes. Similarly, Golovin and Palis [16] introduced a robust control approach for active damping of elastic structural vibrations in gantry cranes. Yongming *et al.* [17] investigated the impact of vertical deformations in cranes on antisway control with a novel three-mass, three-degree-of-freedom elastic dynamic model of the trolley system to address sway. During crane operations, disturbances (arising from sensor measurement errors and environmental conditions) are stochastic and fully accounted for in normal control designs.

Therefore, investigating intelligent control solutions for mitigating load sway in STS crane operations has become a crucial task. This study develops a Deep learning-based Model Predictive Control (DMPC) to enhance the accuracy of control signals during crane operations, thereby reducing load sway. Specifically, a state prediction model for the STS crane is constructed using a Long Short-Term Memory (LSTM) neural network to accurately estimate both the system states and the payload swing angle. The predicted states $\hat{x}(k+1)$ are provided as inputs to the DMPC controller, which computes the quality control forces by an optimization function. Feasible results provided from two testing scenarios, in comparison with comparison approaches, confirm the effectiveness of the proposed solution.

The remainder of this paper is organized as follows: Section 2 presents the dynamic model of the STS crane, providing the mathematical foundation for controller design. Section 3 describes the DMPC controller design, in which the LSTM network is employed to accurately predict the system states, thereby enabling optimization of the control force through the DMPC framework. Section 4 expresses the experimental results and performance evaluation of the DMPC controller under two testing scenarios. Finally, Section 5 summarizes the conclusions of this work and outlines directions for future study.

## 2. The STS crane model

During the operation of STS cranes, load sway is primarily induced by the simultaneous movement of the lifting or lowering of the container. The goal of this study is to design an effective controller to minimize container sways, thereby enhancing productivity and ensuring operational safety. The STS kinematic model includes two main components: the trolley-payload system and the fixed supporting structure, as represented in Figure 2. In the case of ideal conditions, the friction force (translation mechanisms, and the rails), cable elasticity, and external disturbances are neglected. Based on Newton's theory II [18], the acting force of the trolley along the x-axis can be expressed as follows:

$$M_C \frac{d^2x}{dt^2} = u + Fsin\theta \tag{1}$$

The force exerted by the payload is defined as

$$M_L \frac{d^2(x + lsin\theta)}{dt^2} = -Fsin\theta \tag{2}$$

In addition, the trolley force with respect to the motion along the y-axis can be described as follows:

$$Fcos\theta + M_C g = 0 \tag{3}$$

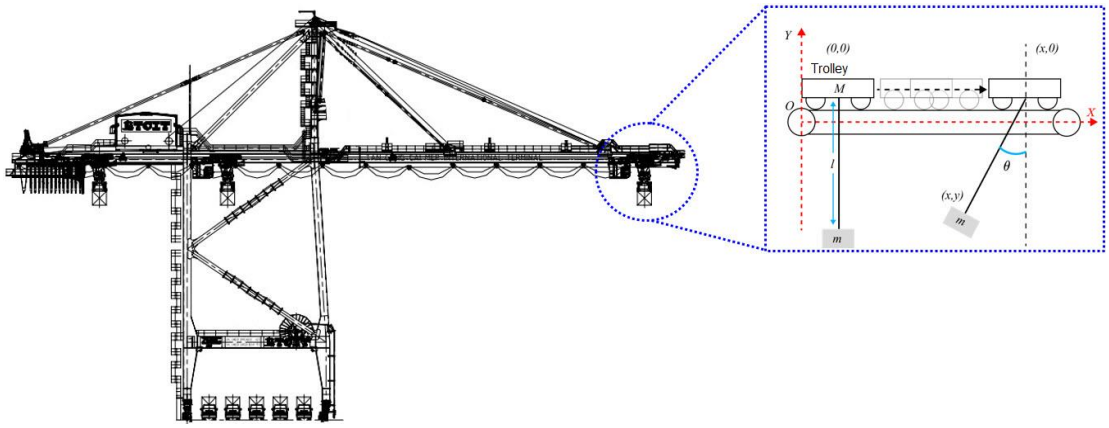


**Figure 2.** Structure of the ship-to-shore crane

The force associated with the payload is rewritten by

$$M_C \frac{d^2x}{dt^2} + M_L \frac{d^2(x + lsin\theta)}{dt^2} = u \tag{4}$$

where $M_L$ denotes the mass of the lifted payload, and $M_C$ represents the mass of the trolley, with $\theta$ being the sway angle of the payload. The parameter $l$ corresponds to the cable length, while $x$ denotes the displacement of the trolley. To transport the payload from the vessel to the quay, the dynamical system is subjected to the trolley control force $u$ and the cable tension force $F$. By transforming equations (1), (2), (3), and (4) with $sin\theta \approx X$ and $cos\theta \approx Y$, the dynamic equations governing the trolley–payload system can be expressed as follows:

$$\begin{cases} \ddot{x} = \dfrac{u + M_L gX(l\theta^2 + gY)}{M_C + M_L X^2} \\ \ddot{\theta} = -\dfrac{uY + M_L X(g + l\theta^2 Y) + M_C gX}{l(M_C + M_L X^2)} \end{cases} \tag{5}$$

$$\dot{x} = \begin{bmatrix} \dot{x_1} \\ \dot{x_2} \\ \dot{x_3} \\ \dot{x_4} \end{bmatrix} = \begin{bmatrix} x_2 \\ \dfrac{u + M_L gX(l\theta^2 + gY)}{M_C + M_L X^2} \\ x_4 \\ -\dfrac{uY + M_L X(g + l\theta^2 Y) + M_C gX}{l(M_C + M_L X^2)} \end{bmatrix} \tag{6}$$

To enable the analysis and design of the anti-sway controller, the operation of the container transfer process from the vessel to the quay must be linearized around the stable operating point. At this equilibrium point, equation (6) can be linearized and represented in the following form:

$$\begin{bmatrix} \ddot{x} \\ \ddot{\theta} \end{bmatrix} = \begin{bmatrix} \dfrac{u + M_L g\theta}{M_C} \\ -\dfrac{u + M_L g\theta + M_C g\theta}{lM_C} \end{bmatrix} \tag{7}$$

$$= \begin{bmatrix} 0 & \dfrac{M_L}{M_C} g \\ 0 & -\dfrac{M_L + M_C}{lM_C} g \end{bmatrix} \begin{bmatrix} x \\ \theta \end{bmatrix} + \begin{bmatrix} \dfrac{1}{M_C} \\ -\dfrac{1}{lM_C} \end{bmatrix} u$$

The linearized system can be expressed as

$$\begin{cases} \dot{x}(t) = Ax(t) + Bu(t) \\ y = Cx + Du \end{cases} \tag{8}$$

Substituting (7) into (8), the state equation representing the trolley–payload system is given by

$$\dot{x} = \begin{bmatrix} 0 & 1 & 0 & 0 \\ 0 & 0 & \dfrac{M_L g}{M_C} & 0 \\ 0 & 0 & 0 & 1 \\ 0 & 0 & \dfrac{-(M_C + M_L)g}{M_C l} & 0 \end{bmatrix} \begin{bmatrix} x_1 \\ x_2 \\ x_3 \\ x_4 \end{bmatrix} + \begin{bmatrix} 0 \\ \dfrac{1}{M_C} \\ 0 \\ \dfrac{-1}{M_C l} \end{bmatrix} u \tag{9}$$

$$\begin{bmatrix} y_1 \\ y_2 \end{bmatrix} = \begin{bmatrix} 1 & 0 & 0 & 0 \\ 0 & 0 & 1 & 0 \end{bmatrix} \begin{bmatrix} x_1 \\ x_2 \\ x_3 \\ x_4 \end{bmatrix} + \begin{bmatrix} 0 \\ 0 \end{bmatrix} u \tag{10}$$

*Remark 1:* In the case of the trolley moving, environmental disturbances combined with drive system errors induce sways of the payload, thereby causing a collision for the STS crane. Consequently, reduction of the payload sway angle becomes both essential and practically significant.

The input $u$ consists of the force generated by the control signal $\tau_{MPC}$ and the force exerted by the environment $\tau_e$. In this study, external environmental disturbances cannot be neglected. It is necessary to account for the forces and moments generated by wind. The wind-induced forces and moments in surge, sway $\tau_e = [X_{wind}, Y_{wind}]$, are expressed as

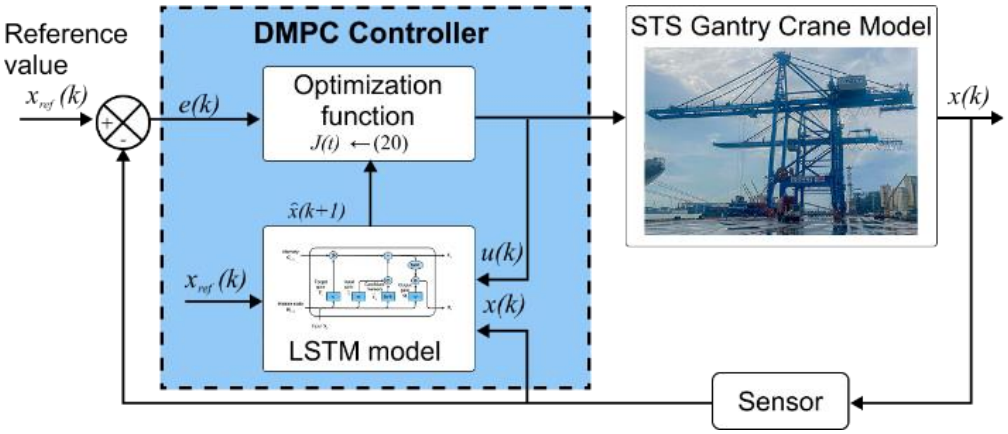


**Figure 3.** Structure of the DMPC controller for sway reduction of the STS crane

$$\begin{cases} X_{wind} = \frac{1}{2} C_X(\alpha_R) \rho_a V_R^2 A_T \\ Y_{wind} = \frac{1}{2} C_Y(\alpha_R) \rho_a V_R^2 A_T \end{cases} \quad (11)$$

therein $C_X$ and $C_Y$ are the wind force coefficients, $\rho_a$ is the air density, $A_T$ and $A_L$ are the frontal and lateral, $V_R$ is the relative wind speed, and $\alpha_R$ is the relative wind direction angle.

*Remark 2:* The dynamic model of the STS crane is formulated under explicit simplifying assumptions: the system is represented in a two-dimensional plane, lateral structural vibrations are excluded, and the payload is modeled as a concentrated point mass. Friction, cable elasticity, and external disturbances are neglected in the baseline model to facilitate controller design. Therefore, the proposed approach is evaluated within a limited operating range, focusing on sway angles of 0.3 to 0.5 rad and payload masses between 15 and 25 tons.

## 3. Developing the deep learning-based model predictive control

### 3.1. Phases and Objectives

In this study, the LSTM network [19-20] predicts the future operation state of the STS crane, denoted as $\hat{x}(k+1)$, based on the current state $x(k)$, and control input $u(k)$. Accordingly, the LSTM serves as a data-driven dynamic model, providing essential input to the MPC controller for accurate prediction and determination of the control signal value. The proposed DMPC solution is structured into three stages as follows:

- *Stage 1:* Developing the STS crane model in the MATLAB 2024a to enable the implementation of control strategies for sway reduction.
- *Stage 2:* Constructing a prediction model based on an LSTM neural network to estimate the subsequent state of STS crane operations.
- *Stage 3:* Designing the DMPC controller, in which the prediction model (at Stage 2) determines the precise control force through the optimization function $J(k)$.

The DMPC approach incorporates the LSTM model as an independent function to simulate the crane's future behavior over a prediction horizon $N_p$. At each time step, the controller compares the predicted state with the reference to compute the error and subsequently formulates an optimization problem to obtain the optimal sequence of control signals within the control horizon $N_c$. The proposed solution's objective is to minimize load sway to guarantee the STS's stable condition.

### 3.2. The LSTM neural network

Recurrent neural networks (RNNs) are time-dependent architectures that have been widely applied in various domains, such as natural language processing [21], and particularly in time-series data analysis [22]. Within their recurrent structure, each neural unit receives an input $x_t$ to compute the corresponding hidden state $h_t$, while the recursive connections enable information to propagate from the current step to subsequent steps. The LSTM architecture enhances this process by selectively retaining relevant information for prediction and discarding irrelevant data. The structure of the LSTM network is described in Figure 3.

In this LSTM structure, $x_t$ denotes the input, with $h_{t-1}$ being the output of the previous layer. The term $f_t$ corresponds to the forget gate output, and $\sigma$ denotes the Sigmoid activation function [23-24], which serves as the output of the input gate. Furthermore, $\widetilde{C}_t$ represents the output of the candidate gate, with tanh denoting the hyperbolic tangent function, and $C_t$ being the output of the memory cell. The LSTM network determines which

information should be discarded from the cell state through the forget gate. Subsequently, the previous output $h_{t-1}$ and the current input $x_t$ are processed to generate a nonlinear mapping via the sigmoid function, thereby defining the vector $f_t$ associated with the cell state $C_{t-1}$.

$$f_t = \sigma(W_f[h_{t-1}, x_t] + b_f) \quad (12)$$

where $W_f$ denotes the weight matrix and $b_f$ represents the bias of the forget gate. The input gate employs the sigmoid activation function [17] to regulate the amount of new information incorporated at the current time step. The $tanh$ layer generates a vector of candidate values that are subsequently added to the cell state, expressed as follows:

$$i_t = \sigma(W_i[h_{t-1}, x_t] + b_i) \quad (13)$$

$$\widetilde{C_t} = tanh(W_C[h_{t-1}, x_t] + b_i) \quad (14)$$

therein, $W_i$ expresses the weight matrix of the input gate, and $b_i$ represents its bias. In addition, $W_C$ is the weight matrix of the candidate gate, with $b_C$ denoting its bias. Accordingly, the cell state is updated as follows:

$$C_t = f_t * C_{t-1} * i_t * \widetilde{C_t} \quad (15)$$

The output is computed based on the cell state, as represented in (16). The cell state is determined via the hyperbolic tangent function (ranging from −1 to 1) and multiplied by the output of the sigmoid gate, as follows:

$$o_t = \sigma(W_o[h_{t-1}, x_t] + b_o) \quad (16)$$

$$h_t = o_t * \tanh(C_t) \quad (17)$$

for $o_t$ denotes the output gate, with $W_o$ being the weight matrix and $b_o$ the corresponding bias.

## 3.3. Designing the DMPC for STS crane sway reduction

The LSTM network input consists of the vector $x(k)$, which includes the state variables $(x_{1k}, x_{2k}, x_{3k}, x_{4k})$, with the control input $u(k)$ representing the external force applied to the system, as expressed in (10). Accordingly, the subsequent predicted output is computed through the LSTM model as follows:

$$\hat{x}(k+1) = f_{LSTM}(x(k), u(k)) \quad (18)$$

The predicted value $\hat{x}(k+1)$ is integrated into the MPC framework [25] to estimate the control force for the STS crane, which is expressed as:

$$u(k) = u(k|k), u(k+1|k), \cdots, u(k+N_c-1|k) \quad (19)$$

where $u(k+p \mid k)$ defines the control input at time step $k+p$, computed at the current time $k$. The control signals include the trolley driving force, which regulates the trolley position $x$ and reduces the swing angle $\theta$. Accordingly, the control force can be decomposed by

$$u(k+p \mid k) = [u_x(k+p \mid k), u_\theta(k+p \mid k)]^T \quad (20)$$

for $u_x$ represents the control signal for the horizontal position of the trolley, whereas $u_\theta$ denotes the control signal for attenuating the swing angle $\theta$. The objective of the DMPC controller is to minimize the error between the output path and the desired reference, while simultaneously imposing constraints on both the control force and the variations of the control signals, as follows:

$$J(k) = \sum_{p=1}^{N_p} (\Delta x(k+p|k))^2 + \lambda \sum_{p=0}^{N_c-1} (\triangle u(k+p \mid k))^2 \quad (21)$$

where $\lambda$ is the weighting factor, and $\Delta x(k+p|k) = x_{ref}(k+p \mid k) - \hat{x}(k+p \mid k)$ denotes the tracking error between the desired value at time step $k+p$, referenced from the initial time $k$, and the predicted value $\hat{x}_0(k+p|k)$ computed at the current iteration. Accordingly, the subsequent predicted state $\hat{x}_1(k+p|k)$ within the prediction horizon $k+N$ is expressed as

$$\hat{x}_1(k+i|k) = \hat{x}_0(k+i|k) + a_i\, \Delta\tau(k) \quad (22)$$

It can be expressed in the matrix form as follows:

$$\hat{x}_{N1}(k) = \hat{x}_{N0}(k) + a\Delta\tau(k) \quad (23)$$

In practical operation, the control input signals are constrained by the mechanical structure and the capabilities of the drive mechanism as follows:

$$\tau_{min} < \tau(k) < \tau_{max} \quad (24)$$

whereas $\tau_{min}$ and $\tau_{max}$ denote the limits of the applied force. The DMPC response is adjusted through $\Delta\tau(k)$ as

$$\Delta\tau(k) = d^T[\omega_p(k) - \hat{x}_{P0}(k)] \quad (25)$$

Here, $d^T$ is computed as follows:

$$d^T = c^T(A^TQA + R)^{-1}A^TQ \quad (26)$$

where, $c^T = [1\ 0 \ldots 0]$ and $A_{P\times M} = \begin{bmatrix} a_1 & \cdots & 0 \\ \vdots & \ddots & \\ a_M & \cdots & a_1 \\ \vdots & & \\ a_P & \cdots & a_{P-M+1} \end{bmatrix}$, Q and $R$ denotes the error weighting matrix and the control weighting matrix, respectively.

Accurate determination of the control output ensures stable operation of the STS crane throughout the overall

process, and beter control performance. In DMPC, the controller output is continuously predicted over the control horizon $T_c$, which may result in predicted signals exceeding allowable limits, potentially causing damage to the actuating equipment. The operating process of DMPC are espress in Algorithm 1.

***Algorithm 1:*** *The DMPC operation process*

**Input:** $x(k)$, LSTM model $\theta^*$, $\Delta t$, $Np$, $Nc$, $Q$, $R$, $S$, $m_{max}$

**Output:** Predicted states $\hat{x}(k)$, Optimal control $\tau(k)$

**Initialize:** Constraints $\tau_{min} < \tau(k) < \tau_{max}$

**Initialize:** STS's state $x_{ref}(k+Np \mid k)$

**while** $0 < m < m_{max}$ **do**

  Measuring output $\leftarrow x_0(k+p|k)$

  Estimating state $\hat{x}_1(k+i|k) \leftarrow$ (22)

  Estimating state $\hat{x}(k+1) \leftarrow$ LSTM(U(k),Np)

  Computing contraints $\leftarrow$ (24)

  Computing $J \leftarrow$ (21)

  Sloving optimal $\min J$

  Computing $\Delta\tau(k) \leftarrow$ (25)

  Computing $\tau \leftarrow \Delta\tau(0)$

  Increasing $m \leftarrow m+1$ *and return Step 3*

**end while**

**end**

## 3.4. Stability analysis

In this study, $x(k) = [x, v, \theta, \omega]^{\mathrm{T}}$ expresses the STS's state with $u(k)$ being the control force. In addition, $d_k$ expresses the LSTM prediction error, considered as additive noise. From (18), the STS nonlinear system is rewritten as

$$x(k+1) = f(x(k), u(k)) + d_k \tag{27}$$

In case of $\| d_k \| \leq \bar{d}$, $f$ denotes a continuous nonlinear function, Lipschitz on the constraint domain around $\theta \approx 0$. That is, there exists a constant $L_f > 0$ such that

$$\| f(x_1, u_1) - f(x_2, u_2) \| \leq L_x \| x_1 - x_2 \| + L_u \| u_1 - u_2 \| \tag{28}$$

where $L_x$ and $L_u$ are the Lipschitz constants specific to each variable. The state error is constrained by

$$\| x_{k+1} - f(x_k, u_k) \| \leq L_f \bar{d} \tag{29}$$

In the Lipschitz area, the LSTM prediction error causes only a bounded bias, and the system under DMPC maintains practical stability. Specifically, there exists a Lyapunov function $V(x)$ as

$$V(x(k+1)) - V(x(k)) \leq -\alpha(\| x(k) \|) + \gamma(\bar{d}) \tag{30}$$

therein $\alpha$ represents the rate of decrease in the Lyapunov derivative with $\gamma$ denoting the influence of disturbances on the system, this demonstrates that the state converges locally to a disturbance-invariant set whose radius is proportional to the bounded prediction error $\bar{d}$.

# 4. Results and evaluations

## 4.1. Configuration parameters

The testing cases were conducted in the MATLAB 2024a computational environment, with the parameters of STS are presented in Table 1. The LSTM model was trained by a dataset obtained from the nonlinear dynamics model of the STS crane system. To illustrate the characteristics and scope of the input data, Table 2 presents the representative initialization conditions ($x_0$, $\phi_0$, $u_{\max}$) of 20 sample data sequences out of a total of 200 simulation sequences used for the training process.

Table 1. Structural parameters of the STS crane

| Parameter | Symbol | Value |
|---|---|---|
| Trolley mass | $M$ | 25000 kg |
| Payload mass | $m$ | 50000 kg |
| Cable length | $l$ | 30 m |
| Gravitational acceleration | $g$ | 9.81 m/s² |
| Sampling time | $T_s$ | 0.1 s |
| Number of operational cases | | 200 |
| Duration of each case | | 180 s |

Table 2. Samples of the training data

| No | $x_0$ (m) | $\phi_0$ $(rad)$ | $u_{Max}$ $(N)$ | No | $x_0$ (m) | $\phi_0$ $(rad)$ | $u_{Max}$ $(N)$ |
|---|---|---|---|---|---|---|---|
| 1 | 0.91 | -0.065 | 27.22 | 11 | -0.69 | -0.032 | 15.36 |
| 2 | 1.29 | -0.065 | 26.68 | 12 | -0.53 | 0.039 | 17.70 |
| 3 | 0.27 | 0.049 | 20.52 | 13 | 0.59 | 0.076 | 27.44 |
| 4 | -0.66 | 0.043 | 17.96 | 14 | 0.32 | -0.024 | 23.79 |
| 5 | -0.14 | -0.003 | 17.86 | 15 | -0.01 | 0.045 | 27.16 |
| 6 | -0.49 | 0.042 | 24.11 | 16 | -0.28 | 0.069 | 17.86 |
| 7 | -0.20 | 0.056 | 19.05 | 17 | 0.94 | -0.016 | 23.68 |
| 8 | -0.86 | 0.024 | 17.83 | 18 | 0.26 | 0.022 | 19.74 |
| 9 | -1.61 | -0.053 | 21.62 | 19 | 0.026 | -0.07 | 19.81 |
| 10 | -0.27 | -0.06 | 21.08 | 20 | -0.17 | 0.07 | 25.18 |

Before proceeding with the detailed training using the dataset, we conducted a comparative training experiment using two loss functions: MAE and RMSE. The results obtained after 300 epochs (Figure 4) show that the model using RMSE converged better and achieved lower prediction errors. Therefore, RMSE was chosen as the loss function for training the LSTM model in this study.

The state prediction model was trained with 128 hidden layers, enabling the model to capture the nonlinear dynamic characteristics of the STS crane. The training process utilized the Adam optimization algorithm [26-27], which provides fast and stable convergence, with a learning rate of 0.0001, allowing appropriate weight updates while avoiding large variations.

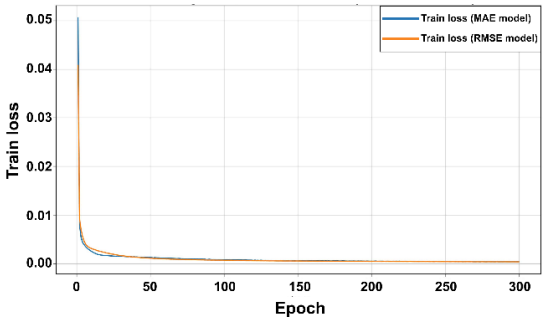


**Figure 4.** Training loss comparisions

Training data was conducted over 20,000 epochs to ensure comprehensive learning from the training dataset. Additionally, a mini-batch size of 32 was used to balance the computational efficiency and stability in parameter updates. The convergence of the model during training is illustrated in Figure 5, showing a steady decrease in the evaluation function after approximately 1,000 epochs. This result indicates that the training process was effective without overfitting. The stable convergence reflects a rational selection of training parameters, particularly the small learning rate and sufficiently large number of epochs, allowing the model to learn deeply from the operational data of the STS crane. The RMSE [28-29] achieved a minimum value of 0.1945.

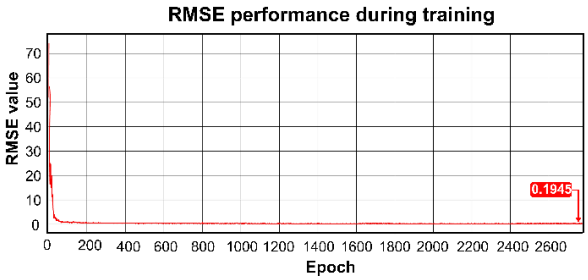


**Figure 5.** Training results of the LSTM network

The authors developed two testing cases: the first case involved varying the load swing angles to evaluate the feasibility of the proposed solution; the second case carried out the proposed approach under increasing container payloads to assess the quality of the control strategy.

The control system is evaluated as stable and effective, with sufficient phase and gain margins, verifying its ability to withstand disturbances and uncertainties, as shown in Figure 6. The results demonstrate that DMPC consistently maintains gain margins above 10dB and phase margins greater than 40°, surpassing standard stability thresholds (GM > 6 dB, PM > 30°). These margins confirm that DMPC provides strong closed-loop stability, effective sway suppression, and reliable adaptability to load variations, validating it as a practical control strategy for STS crane operations.

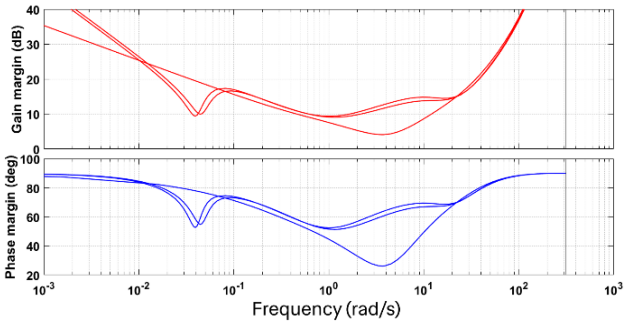


**Figure 6.** Stability analysis by using gain margin and phase margin

## 4.2. Case 1

In the first testing case, the DMPC controller is performed under varying swing angles to assess its precision in control and its effectiveness in reducing load swing, with the STS crane operating at a minimum load of 15 tons. In this testing, the trolley was moved from 0 m to 3 m, with the control velocity computed by the DMPC algorithm based on predictions from the LSTM network. The focus of this case was to monitor the trolley's horizontal position response and the swing angle amplitude of the cable. To evaluate the controller's robustness, three initial swing angles were introduced. These variations represent different levels of initial disturbance, allowing for a comparative analysis of the DMPC, and MPC strategies.

The results, as described in Figure 7, clearly verify the effectiveness of the DMPC controller compared to the MPC [25], particularly in handling load sway and variations in sway angles. The comparison results in Table 3 show that the DMPC has better position control with significantly reduced overshoot, specifically 0.7 % for DMPC compared to 2.07 % for MPC in a sway angle of 0.3 rad. In addition, the proposed solution maintains a low level of 0.74 % to 0.81 % as the sway angle increases, whereas MPC reaches 2.14 % to 2.25 %. The settling error of DMPC is also markedly lower, at only 0.01 m compared to 0.015 m for MPC at 0.3 rad, and 0.026 m versus 0.032 m for MPC at 0.5 rad.

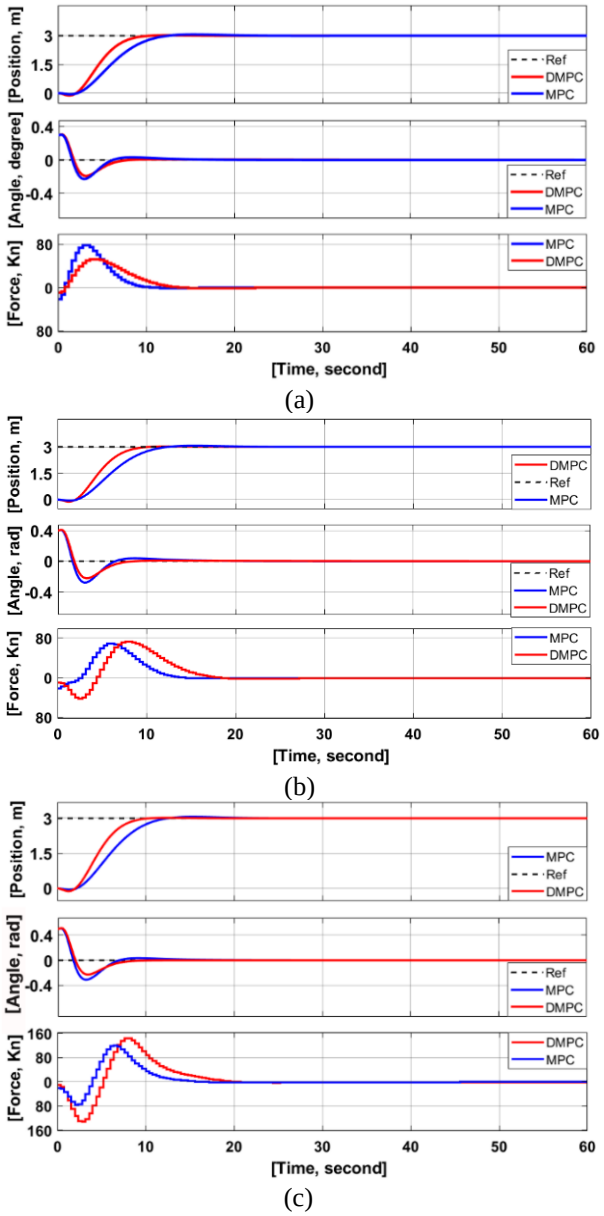


**Figure 7.** Results of case 1 for sway angle: (a) 0.3 rad, (b) 0.4 rad, (c) 0.5 rad

Furthermore, the NNMPC [30] is an approach that integrates neural network-based prediction into the MPC framework, which also shows improved performance over traditional MPC. The comparison results summarized in Table 3 show the changes in the sway angles. At a sway angle of 0.3 rad, NNMPC achieves an overshoot of 0.8 %, slightly higher than DMPC but significantly lower than MPC. Its steady-state error is 0.011 m, and the settling time is 15 s, both better than MPC's 0.015 m and 20 s, respectively. As the sway angle increases to 0.5 rad, NNMPC maintains competitive metrics with 0.82 % overshoot, 0.028 m steady-state error, and 21 s settling time. These results demonstrate that DMPC, owing to the accurate predictive capability of the LSTM model, can compensate sways more effectively.

Table 3. Comparision results for the first case

| Swing angle | DMPC | NNMPC | MPC |
|---|---|---|---|
| Overshoot (%) | | | |
| 0.3 (rad) | 0.7 | 0.8 | 2.07 |
| 0.4 (rad) | 0.74 | 0.76 | 2.14 |
| 0.5 (rad) | 0.81 | 0.82 | 2.25 |
| Steady-state error (m) | | | |
| 0.3 (rad) | 0.01 | 0.011 | 0.015 |
| 0.4 (rad) | 0.015 | 0.017 | 0.021 |
| 0.5 (rad) | 0.026 | 0.028 | 0.032 |
| Settling time (s) | | | |
| 0.3 (rad) | 12 | 15 | 20 |
| 0.4 (rad) | 15 | 17 | 26 |
| 0.5 (rad) | 18 | 21 | 32 |

Moreover, the DMPC exhibits a notable advantage in system stabilization speed. The settling time of DMPC is consistently shorter than that of MPC, with DMPC achieving stability in just 12 s at a sway angle of 0.3 rad, 8 s faster than MPC, and 18 s at 0.5 rad compared to 32 s for MPC. These results indicate that the flexible response and optimized control capability of DMPC allow the system to achieve a stable state. Therefore, the DMPC not only significantly improves position control and reduces overshoot but also demonstrates better effectiveness in minimizing settling error and shortening settling time, even under large sway angle conditions, confirming its high potential for application in an actual STS crane.

## 4.3. Case 2

In the second case, we focus on assessing the adaptability of the proposed control solution under substantial variations in load and impact of environment. The wind parameters acting on the STS include the lateral wind area $A_L = 2.4\,\mathrm{m}^2$, the frontal wind area $A_T = 9.34\,\mathrm{m}^2$. The wind speed is $V_\omega = 2$ m/s with a wind angle of $\beta_\omega = 200°$. This case was designed to emulate actual conditions, in which the container mass is not constant. Specifically, the payload was incrementally increased from 15 tons to 20 tons, and finally to 25 tons. For each load level, the trolley was commanded to move from position 0 m to 3 m, with the velocity determined by the MPC algorithm based on an LSTM prediction model. This case aims to verify the controller's effectiveness in maintaining accurate trolley position control and, importantly, in minimizing cable swing amplitude in case the STS crane changes payloads.

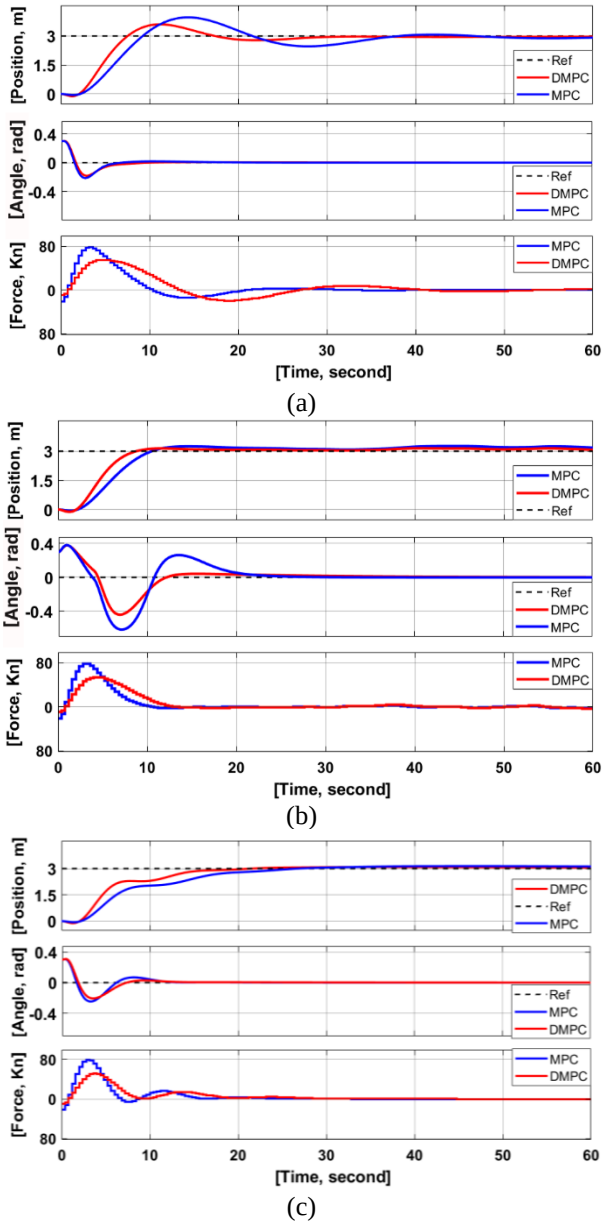


**Figure 8.** The second case results for payloads: (a) 15 ton, (b) 20 ton, (c) 25 ton

The results shown in Figure 8 confirm the effectiveness of the DMPC in controlling the sled position and minimizing the cable sway amplitude when the system is subjected to variations in the load mass. The simulation results presented in Table 4 indicate that the DMPC is better than the MPC [25] and NNMPC [30], especially in stabilizing the load sway and adapting to different loads. The simulation results presented in Table 4 show that the DMPC has a significantly lower overshoot at the 15-ton load level; specifically, the DMPC is lower than the MPC by 1.1 %. At the 25-ton level, the DMPC also maintains a significantly lower overshoot of 4.7 % compared to the MPC's 8.3 %, ensuring better accuracy. Furthermore, the steady-state error is also reduced compared with the DMPC, with the 15-ton level having a lower error of about 35.5 % compared to 0.031 m with MPC. At the 20-ton level, the steady-state error of the DMPC solution reaches a low of 0.06 m, expressing a reduction of 0.02 m compared to MPC. At the 25-ton level, the DMPC also results in a low steady-state error of 0.11 m, while NNMPC records overshoots of 2.7 %, 3.8 %, and 5.1 % for payloads of 15, 20, and 25 tons, respectively, that higher than DMPC in each case. Similarly, its steady-state errors of 0.021 m, 0.064 m, and 0.14 m are consistently above those of DMPC. Settling times also favor DMPC, which stabilizes faster across all payloads. These comparisons reinforce that the DMPC offers the most reliable and precise control performance under dynamic load conditions.

Table 4. Comparision results of the second case

| Payload | DMPC | NNMPC | MPC |
|---|---|---|---|
| Overshoot (%) | | | |
| 15 (ton) | 2.4 | 2.7 | 5.3 |
| 20 (ton) | 3.6 | 3.8 | 7.4 |
| 25 (ton) | 4.7 | 5.1 | 8.3 |
| Steady-state error (m) | | | |
| 15 (ton) | 0.02 | 0.021 | 0.031 |
| 20 (ton) | 0.06 | 0.064 | 0.08 |
| 25 (ton) | 0.11 | 0.14 | 0.16 |
| Settling time (s) | | | |
| 15 (ton) | 20 | 24.2 | 26 |
| 20 (ton) | 23.3 | 25 | 28.7 |
| 25 (ton) | 26.5 | 27 | 30.6 |

Furthermore, the DMPC achieves significantly faster settling times than MPC at the 15-ton level, meeting the stability in 6 s faster than MPC.At the 20-ton level, the reduction is 5.4 s, and the proposed solution stabilizes in 26.5 s compared to 30.6 s for MPC at the 25-ton level. These results indicate the controller's flexible response and rapid stabilization capability in dynamic operating environments, satisfying the conditions stated in Remarks 1, and 2. Overall, the findings confirm the high potential of the DMPC solution for practical application in the STS crane. For a payload of 20 tons, the total computation time was measured as 18.7528 seconds during a 60-second control process with a sampling time of 0.01 s. This corresponds to an average computation time of approximately 3.1 ms per step, which is significantly lower than the actual control cycle for the STS crane (5-20 ms). These results confirm that the proposed DMPC can operate in real time without introducing delays that would affect system stability or control performance.

## 5. Conclusion

This study developed an LSTM neural network integrated with MPC to accurately control the operation of STS cranes, aiming at reducing the sway amplitude and improving the control response. The LSTM neural network calculates a state prediction model in predicting the load sway angle and winch displacement amplitude. Thus, the STS predicted state is used as input for the DMPC controller to determine the winch control value, which reduces the load sway angle through the optimization function. The results from the two testing cases indicate that the DMPC can adapt to load variations while maintaining stability despite changes in sway angle and payload. In the future, the application of deep learning-based MPC for reducing crane load sway angles needs verification through various testing cases, and the wind impact on sway angle changes should be considered. Furthermore, this paper focuses on the design and experimental evaluation of a DMPC controller combine with LSTM prediction. Theoretical proofs of Lyapunov stability, repeatability, and analysis of prediction error effects will be directions for further research.

## References


[1] Zhang S, He X, Zhu H, Chen Q, Feng Y. Partially saturated coupled-dissipation control for underactuated overhead cranes. Mechanical Systems and Signal Processing. 2020; 136: 106449. doi: 10.1016/j.ymssp.2019.106449

[2] Lu B, Fang Y, Sun N. Sliding mode control for underactuated overhead cranes suffering from both matched and unmatched disturbances. Mechatronics. 2017; 47: 116–125. doi: 10.1016/j.mechatronics.2017.09.006

[3] Chen H, Fang Y, Sun N. An adaptive tracking control method with swing suppression for 4-dof tower crane systems. Mechanical Systems and Signal Processing. 2019; 123: 426–442. doi: 10.1016/j.ymssp.2018.11.018

[4] Zhong B, Zhan R. Load's damping swing by trolley's driving force control for overhead or gantry crane. Advanced Materials Research. 2012; 346: 875–881. doi: 10.4028/www.scientific.net/AMR.346.875

[5] Martin IA, Irani RA. A generalized approach to anti-sway control for shipboard cranes. Mechanical Systems and Signal Processing. 2021;148: 107168. doi: 10.1016/j.ymssp.2020.107168

[6] Suvorov VA, Bahrami MR, Akchurin EE, Chukalkin IA, Ermakov SA, Kan S A. Anti sway tuned control of gantry cranes. SN Applied Sciences. 2021; 3(8): 729. doi: 10.1007/s42452-021-04719-w

[7] Chang CY, Hsu KC. An enhanced adaptive sliding mode fuzzy control for positioning and anti-swing control of the overhead crane system. IEEE International Conference on Systems, Man and Cybernetics. 2007; 2: 992-997. doi: 10.1109/ICSMC.2006.384529

[8] Smoczek J, Szpytko J. Particle swarm optimization-based multivariable generalized predictive control for an overhead crane. IEEE/ASME Transactions on Mechatronics. 2017; 22(1): 258–268. doi: 10.1109/TMECH.2016.2598606

[9] Kusznir T, Smoczek J. Nonlinear Model Predictive Control with Evolutionary Data-Driven Prediction Model and Particle Swarm Optimization Optimizer for an Overhead Crane. Applied Sciences. 2024; 14(12):5112. doi: 10.3390/app14125112

[10] Zhang P, Wu HN, Chen RP, Chan THT. Hybrid meta-heuristic and machine learning algorithms for tunneling-induced settlement prediction: A comparative study. Tunnelling and Underground Space Technology. 2020; 99: 103383. doi: 10.1016/j.tust.2020.103383

[11] Dang XK, Koboević Z, Nguyen HLP, Do VD, Ly S. Artificial Neural Network for Improving the Motion Control Quality of Underwater Remotely Operated Vehicle. NAŠE MORE. 2025; 72(2): 39 - 48. doi: 10.17818/NM/2025/2.1

[12] Liu T, Tang X, Wang H, Yu H, Hu X. Adaptive hierarchical energy management design for a plug-in hybrid electric vehicle. IEEE Transactions on Vehicular Technology. 2019; 68(12): 11513–11522. doi: 10.1109/TVT.2019.2926733

[13] Raj Priyadarshini R, Sivakumar N. Failure prediction, detection & recovery algorithms using MCMC in tree-based network topology to improve coverage and connectivity in 3D-UW environment. Applied Acoustics. 2020; 158: 107053. doi: 10.1016/j.apacoust.2019.107053

[14] Li S, Song X, Lu H, Zeng L, Shi M, Liu F. Friend recommendation for cross marketing in online brand community based on intelligent attention allocation link prediction algorithm. Expert Systems with Applications. 2020; 139: 112839. doi: 10.1016/j.eswa.2019.112839

[15] Zhang M, Zhang Y, Chen H, Cheng X. Model-independent PD-SMC method with payload swing suppression for 3D overhead crane systems. Mechanical Systems and Signal Processing. 2019;129: 381–393. doi: 10.1016/j.ymssp.2019.04.046

[16] Golovin I, Palis S. Robust control for active damping of elastic gantry crane vibrations. Mechanical Systems and Signal Processing. 2019; 121: 264–278. doi: 10.1016/j.ymssp.2018.11.005

[17] Yongming B, Jiange Y, Xiaolei X, Lu W, Lishan Z. Research on elastic dynamic model of trolley system for anti-sway control system of bridge crane. Procedia CIRP. 2018; 78: 285–288. doi: 10.1016/j.procir.2018.08.325

[18] Wang L, Zhang Q, Sun Y, Qing X. Moving Load Identification for STS Cranes Based on Hybrid Weighted Regularization Method. In Journal of Physics: Conference Series. 2020; 1549: 1-10. doi: 10.1088/1742-6596/1549/4/042109

[19] Jung M, Costa Mendes PR, Önnheim M, Gustavsson E. Model predictive control when utilizing LSTM as dynamic models. Engineering Applications of Artificial Intelligence. 2023; 123: 106226. doi: 10.1016/j.engappai.2023.106226

[20] Jeong SK, Ji DH, Oh JY, Seo JM, Choi HS. Disturbance learning controller design for unmanned surface vehicle using LSTM technique of recurrent neural network. Journal of Intelligent and Fuzzy Systems. 2021; 40: 8001–8011. doi: 10.3233/JIFS-189622

[21] Chauhan A, Kukkar Y, Nagrath P, Gupta K, Hemanth JD. Integrating LSTM and NLP techniques for essay generation. Intelligent Decision Technologies. 2024; 18(1): 571–584. doi: 10.3233/IDT-230424

[22] Pham TA, Dang XK, Koboević Z, Do VD, Pham TDA. Maritime data mining for marine safety based on deep learning: Southern Vietnam case study. NAŠE MORE. 2024; 71: 21–29. doi: 10.17818/NM/2024/1.4

[23] Cheng H, Xie Z, Shi Y, Xiong N. Multi-step data prediction in wireless sensor networks based on one-dimensional CNN and bidirectional LSTM. IEEE Access. 2019; 7: 117883–117896. doi: 10.1109/ACCESS.2019.2937098

[24] Dang XK, Corchado JM, Le VV, Do VD. Non-parametric Vibration-based Structural Damage Detection for Coastal

Structures: Multi-Dimension to Single Input Convolutional Neural Network Approach. Advances in Electrical and Computer Engineering. 2024; 24(4): 3-18. doi: 10.4316/AECE.2024.04001

[25] Cao Y, Li T, Hao L. Nonlinear model predictive control of shipboard boom cranes based on moving horizon state estimation. Journal of Marine Science and Engineering. 2023; 11(1): 1–17. doi: 10.3390/jmse11010004

[26] Chandriah KK, Naraganahalli RV. RNN/LSTM with modified Adam optimizer in deep learning approach for automobile spare parts demand forecasting. Multimedia Tools and Applications. 2021; 80(17): 26145–26159. doi: 10.1007/s11042-021-10913-0

[27] Redwannewaz AA, Alam T, Murad Reis G, Bobadilla L, Smith RN. Long-Term Autonomy for AUVs Operating under Uncertainties in Dynamic Marine Environments. IEEE Robotics and Automation Letters. 2021; 6(4): 6313–6320. doi: 10.1109/LRA.2021.3091697

[28] Wen X, Li W. Time series prediction based on LSTM-Attention-LSTM model. IEEE Access. 2023; 11: 48322–48331. doi: 10.1109/ACCESS.2023.3276628

[29] Dang XK, Nguyen TD, Do VD, Nguyen NT. Control Parameter Optimization of the Automatic Voltage Regulator for Marine Synchronous Generator Based on Genetic. In 11th International Conference on Coastal and Ocean Engineering (ICCOE-2024). 2024: 442. doi: 10.1007/978-981-96-0181-3_40

[30] Jakovlev S, Eglynas T, Voznak M. Application of Neural Network Predictive Control Methods to Solve the Shipping Container Sway Control Problem in Quay Cranes. IEEE Access. 2021; 9:78253-78265. doi: 10.1109/ACCESS.2021.308392